HHS Public Access

Author manuscript

Nat Cell Biol. Author manuscript; available in PMC 2014 January 01.

Published in final edited form as:

Nat Cell Biol. 2013 July ; 15(7): 807–817. doi:10.1038/ncb2767.

The perivascular niche regulates breast tumor dormancy

Cyrus M. Ghajar[1], **Héctor Peinado**[2,3], **Hidetoshi Mori**[1], **Irina R. Matei**[2,3], **Kimberley J. Evason**[4], **Hélène Brazier**[2,3], **Dena Almeida**[3], **Antonius Koller**[6], **Katherine A. Hajjar**[2,3], **Didier Y.R. Stainier**[5,10], **Emily I. Chen**[6,7], **David Lyden**[2,3,8,9], and **Mina J. Bissell**[1]

[1]Life Sciences Division, Lawrence Berkeley National Laboratory, Berkeley, CA 94720, USA

[2]Department of Pediatrics, Weill Cornell Medical College, New York, NY 10021, USA

[3]Department of Cell and Developmental Biology, Weill Cornell Medical College, New York, NY 10021, USA

[4]Department of Pathology, University of California, San Francisco, San Francisco, CA 94158, USA

[5]Department of Biochemistry and Biophysics, University of California, San Francisco, San Francisco, CA 94158, USA

[6]Stony Brook University Proteomics Center, School of Medicine, Stony Brook, NY 11794, USA

[7]Department of Pharmacological Sciences, Stony Brook University, Stony Brook, NY 11794, USA

[8]Department of Pediatrics, Memorial Sloan-Kettering Cancer Center, New York, NY 10021, USA

[9]Champalimaud Metastasis Programme, Lisbon, Portugal

Abstract

In a significant fraction of breast cancer patients, distant metastases emerge after years or even decades of latency. How disseminated tumor cells (DTCs) are kept dormant, and what ‘wakes them up’, are fundamental problems in tumor biology. To address these questions, we utilized metastasis assays in mice to show that dormant DTCs reside upon microvasculature of lung, bone marrow and brain. We then engineered organotypic microvascular niches to determine whether endothelial cells directly influence breast cancer cell (BCC) growth. These models demonstrated that endothelial-derived thrombospondin-1 induces sustained BCC quiescence. This suppressive cue was lost in sprouting neovasculature; time-lapse analysis showed that sprouting vessels not

Correspondence to: Cyrus M. Ghajar; Mina J. Bissell.

[10]Current address: Department of Developmental Genetics, Max Planck Institute for Heart and Lung Research, Bad Nauheim, Germany

Author Contributions

C.M.G., D.L. and M.J.B. conceived of the study. C.M.G., H.P., I.M. and H.B. conducted animal studies and analyzed resulting data. C.M.G., K.J.E and D.Y.R.S. planned and executed zebrafish experiments. D.A. and K.A.H. lent expertise in the retinal neovascularization model. C.M.G. and H.M. collected and analyzed data, and H.M. also provided conceptual advice. A.K. and E.I.C. conducted LC-MS/MS analysis and analyzed data. C.M.G. and M.J.B. wrote the manuscript. All authors read and critiqued the manuscript extensively.

Competing Financial Interests

The authors declare no competing financial interests.

only permit, but *accelerate* BCC outgrowth. We confirmed this surprising result in dormancy models and in zebrafish, and identified active TGF-β1 and periostin as tumor-promoting, endothelial tip cell-derived factors. Our work reveals that stable microvasculature constitutes a 'dormant niche,' whereas sprouting neovasculature sparks micrometastatic outgrowth.

Introduction

It has been difficult if not impossible to predict if and when metastases will occur[1]. The reason is that although the metastatic cascade is depicted typically as a linear process, in reality it is anything but. Some patients may experience metastatic relapse within months whereas others go several years or even decades without distant recurrence[1–4]. The recent discovery of tumor promoting milieus (referred to as metastatic niches[5–7]) established at distant sites prior to- or upon- the arrival of disseminated tumor cells (DTCs) could explain the population that relapses early. But in late relapsing populations, what tumor cells do from the time of dissemination to the time they become clinically detectable is an outstanding question. Studies in mice and analysis of human clinical specimens revealed that single- or small clusters of DTCs may persist long-term in a state of quiescence[2,8–10]. Precisely where these cells reside, how they are induced into a dormant state and what eventually causes them to 'awaken' remain perplexing mysteries in tumor biology. Solving these problems is key to designing therapies that prevent relapse by either sustaining tumor dormancy or by selectively killing off dormant cells with minimal damage to normal tissues[11].

We have long argued and provided evidence that basement membrane (BM), in particular laminin-111, provides a hospitable microenvironment that allows mammary epithelial cell survival, quiescence and resistance to cytotoxic agents[12–17], three properties commonly associated also with dormant DTCs[18]. Thus, we suspected that BM was a major component of the 'dormant niche' in distant organs. Given that breast cancer cells (BCCs) must take a haematogenous route to arrive at sites where breast tumors metastasize most often (i.e., lung, bone marrow (BoMa), brain and liver)[19], the microvascular BM would be the first of its kind encountered by tumor cells as they disseminate to these tissues. Therefore, we reasoned that endothelial cells (ECs) — and factors deposited within their surrounding BM— may be a prime player within the dormant niche.

To test this hypothesis, we utilized two mouse models of human breast cancer metastasis and discovered that dormant DTCs reside upon the microvasculature of lung, BoMa and brain. By creating organotypic models of lung- and BoMa- microvascular niches, we demonstrated that ECs induce and sustain BCC quiescence. Proteomic and functional analyses of proteins deposited in organotypic microvascular niches identified thrombospondin-1 (TSP-1) as an endothelium-derived tumor suppressor. Importantly, TSP-1 was diminished near sprouting neovasculature, suggesting that tumors may escape growth regulation in this 'sub-niche'. Time-lapse analysis confirmed that tumor growth was not just permitted, but in fact accelerated around neovascular tips, which we show are rich in tumor-promoting factors such as active TGF-β1 and periostin (POSTN). These findings establish a paradigm of differential regulation of DTC dormancy and relapse by distinct endothelial

sub-niches, and suggest that preserving vascular homeostasis is critical to maintaining dormancy of DTCs.

Results

Dormant DTCs reside on microvascular endothelium

To determine whether dormant DTCs occupy a specific niche, we searched first for DTCs lacking expression of the cell cycle marker, Ki67 in a spontaneous metastasis model of breast cancer[20]. Tumors resulting from orthotopic injection of MDA-MB-231, a bona fide metastatic BCC line expressing GFP-luciferase, were resected after 3 weeks (V_{avg}= 0.5 cm^3, Fig. 1a). Surviving mice that did not experience relapse at the primary site were sacrificed 6 weeks later. Bioluminescence of dissected visceral organs confirmed that BCCs disseminated to the canonical target organs— lung, bone, liver, and brain[21] (Fig. 1a). In contrast to the resected primary tumors, in which BCCs proliferated actively whether nearby tumor vasculature or not (Fig. 1b), we found small clusters of GFP-positive/Ki67-negative BCCs residing directly on microvascular endothelium of both lung (Fig. 1c) and BoMa (Fig. 1d).

This observation was confirmed also with a weakly metastatic BCC line (mCherry-HMT-3522-T4-2[22]), which was injected intra-cardially to facilitate dissemination to all target organs (Fig. 1e). Eight weeks after injection into the left ventricle of NOD-SCID mice, small clusters of mCherry-positive (false-colored green)/Ki-67-negative T4-2 cells were found residing perivascularly in murine lung (Fig. 1f), BoMa (Fig. 1g) and brain (Fig. 1h). The consistent discovery of quiescent DTCs residing perivascularly— 6 weeks after resection of the primary tumor in the first model, and 8 weeks post-injection in the second model— suggested that endothelium might play an active role in regulating tumor dormancy.

Organotypic microvascular niches demonstrate that endothelial cells induce sustained quiescence of BCCs

Determining whether microvascular endothelium could directly influence tumor cell quiescence necessitated lung- and BoMa-like designer microenvironments that would allow quantitative assessment of human BCC growth in the presence or absence of a microvascular network. There are considerable hurdles to engineering such models. For example, whereas ECs do not survive in serum- and cytokine-free medium (SFM), the addition of exogenous factors could mask the effects of EC-derived “angiocrine” factors on tumor growth[23–25].

To overcome this limitation, primary human umbilical vein endothelial cells (HUVECs) were transduced with a lentiviral construct containing the human adenoviral *E4ORF1* gene[24], which enables HUVECs to survive[24] and form sustainable microvascular networks in SFM (Supplemental Fig. 1). *E4ORF1*-HUVECs (E4-ECs)-expressing mCherry self-assembled into robust three-dimensional (3D) microvascular networks[26] over 7 days when cultured with fibroblasts from lung (LFs) or with BoMa mesenchymal stem cells (MSCs). We then compared the growth of yellow fluorescent protein (YFP)-expressing T4-2 cells

seeded sparsely in SFM onto lung- and BoMa-like microvascular niches or onto only the corresponding stroma (i.e., LFs or MSCs) after an additional 10 days (Fig. 2a). Whereas T4-2 cells grew extensively on lung and BoMa stroma, growth of T4-2 cells on organotypic microvascular niches was reduced drastically (3-fold in lung-like- and 5-fold in BoMa-like-microenvironments; Fig. 2b–d). Similar results were obtained also with a luminal, estrogen receptor-positive (ER^+) BCC line (MCF-7) (Supplemental Fig. 2a, b). Highly metastatic MDA-MB-231 cells displayed the same trend; in particular, cells adherent to microvasculature were Ki67-negative (Supplemental Fig. 2c–e). Ki67 immunofluorescence (Fig. 2b, inset) revealed further that the vast majority of T4-2 cells seeded in organotypic microvascular niches became quiescent (77.4% Ki67-negative clusters in lung-like niche and 88.1% in BoMa-like niche; Fig. 2e, f). Importantly, this was not a transient phenotype, as microvasculature-associated tumor clusters remained dormant by and large, as opposed to BCCs cultured only on lung or BoMa stroma (Fig. 2g–j). Thus, our organotypic models recapitulated our *in vivo* findings and allowed us to pinpoint ECs as a prime regulator of DTC quiescence in lung and BoMa. We next sought to identify endothelium-derived factor(s) underlying this effect.

Thrombospondin-1 is deposited around mature endothelium and is an angiocrine tumor suppressor

We noted consistently that whereas the bulk of quiescent tumor clusters remained on or near microvascular endothelium in our culture models, those that had seeded— or strayed— to the edge of a well and off of microvasculature typically underwent drastic expansion (Supplementary Fig. 3a; inset shows that all clusters originated from single cells). This observation hinted that the putative angiocrine tumor suppressor(s) was not freely diffusible. Indeed, medium conditioned daily by microvascular niche cultures did not reduce T4-2 cell growth on lung stroma when compared to control conditions (Supplementary Fig. 3b, c). Accordingly, to identify factors deposited locally by ECs that could suppress tumor cell growth, we performed comparative proteomics on decellularized extracellular matrix (ECM) from lung- and BoMa-like microvascular niches (versus their respective stroma). A number of extracellular factors were upregulated in organotypic microvascular niches (Fig. 3a). Among these potential angiocrine tumor suppressors, TSP-1 caught our attention because: i) TSP-1 was expressed at higher levels in both organotypic lung- and BoMa-microvascular niches compared to stroma alone (Fig. 3a), and ii) TSP-1 overexpression in BCCs was shown previously to suppress metastatic outgrowth in lung[27]. However, these anti-tumor effects were attributed to the anti-angiogenic activity of TSP-1[27]. The possibility that TSP-1 could function to directly suppress tumor cell growth (particularly from a non-tumor source within the DTC microenvironment) had not been considered[28].

We verified first that TSP-1 was present on lung microvessels associated with dormant DTCs in both spontaneous and experimental metastasis models (Fig. 3b, c). We confirmed also that TSP-1 is expressed in non-tumor bearing mice in the microvascular BM of murine lung (Fig. 3d), bone (Fig. 3e) and brain (Fig. 3f). Similar peri-endothelial localization was observed also in organotypic microvascular niches. To determine whether perivascular TSP-1 is derived primarily from ECs, we utilized a 3D co-culture model consisting of EC-coated microcarrier beads embedded within a fibrin ECM several millimeters away from

overlaid LFs. ECs form robust microvascular networks after 7 days under these conditions[29], and TSP-1 was concentrated within the BM of established microvessels (Fig. 3g, h). Gain-of-function studies confirmed that TSP-1 was sufficient to suppress BCC growth on lung stroma in the absence of endothelium (Fig. 3i). Additionally, pre-treatment with a TSP-1 blocking antibody to interfere with T4-2 cell adhesion to TSP-1 within lung-like microvascular niches resulted in significantly increased tumor cell outgrowth compared to IgG control-treated cultures (Fig. 3j). These gain- and loss- of function experiments, combined with its presence in microvascular BM and its association with dormant DTCs, identified TSP-1 as an angiocrine tumor suppressor.

Neovascular tips accelerate breast tumor cell outgrowth

Because TSP-1 stabilizes microvascular endothelium by inhibiting EC motility and growth[28], it was not surprising to find it expressed surrounding established microvasculature (Fig. 3d–g). However, loss of TSP-1 expression at neovascular tips (Fig. 3g, h) suggested that this physiological 'knockdown' could result in a concomitant loss of tumor suppression within neovascular sub-niches. In support of this idea, we found that quiescent tumor clusters were often associated with stable endothelial stalks (Fig. 4ai; asterisk, and also aii-iv, all from the same culture), whereas actively growing tumor clusters were often surrounded by sprouting neovascular tips (Fig. 4ai; 'T'). Therefore, we hypothesized that these two sub-niches exert differential growth control over BCCs.

Malignant T4-2 cells expressing histone H2B-GFP were seeded on top of microvascular niches and tracked for 72h. Qualitative analysis of time-lapse videos revealed that tumor cells remaining near established vessel stalks divided more slowly than those that encountered neovascular tips (Fig. 4b; Supplemental Videos 1, 2). To perform quantitative analysis, we defined 3 sub-niches: 'neovascular tip' for tumor cells within 50 μm of a sprouting endothelial tip, 'stable endothelium' for tumor cells within 50 μm of established, non-invasive endothelium and 'stroma' for tumor cells >50 μm away from either type of endothelium. We quantified the aggregate time (i.e., dwell time, t_{dwell}) that 229 tumor cells spent in each of these sub-niches before undergoing a single division (division time: t_{div}). Thus, in Figure 4c, the scatter plot represents the fraction of each T4-2 cell's t_{div} spent near stable (red) or neovascular (green) endothelium, or on stroma (black). Pearson correlation analysis revealed that dwell time around stable endothelium ($t_{dwell,\ stable}$) correlated significantly with t_{div} (two-tailed p value= 0.014); i.e., BCCs with longer division times tended to reside longer near established endothelium (Fig. 4c, red trend line). Conversely, tumor cell dwell time around neovascular tips ($t_{dwell,neo}$) *anti-correlated* significantly with t_{div} (two-tailed p value= 0.001; green trend line in Fig. 4c). Importantly, stromal dwell time ($t_{dwell,\ stroma}$) did not correlate with t_{div} (Fig. 4c, black trend line) at all. We extended this analysis further by examining the fastest- ($t_{div} < t_{avg} - SD$) and slowest- ($t_{div} > t_{avg} + SD$) dividing tumor cells and found that the fastest dividing tumor cells resided 2.1-times longer within neovascular sub-niches than around stable endothelium, whereas the slowest dividing tumor cells did the opposite (Fig. 4d).

Our analysis suggested that established endothelium steers BCCs towards a quiescent phenotype, whereas neovascular endothelium accelerates BCC growth. If this were indeed

true, tumor growth should decrease if neovascular tips are depleted prior to tumor cell seeding, and increase if neovascular tip formation is promoted. Consistent with observations from the developing mouse retina[30], reduced expression of endothelial Notch1 via Notch-1 targeting shRNA (Supplemental Fig. 4) led to a hyperbranched network, but with a significant reduction in the number of endothelial tips (Fig. 5a–c). This was to be expected from a 'closed system' (our case), as opposed to an 'open system' (the developing retina[30]). BCC growth followed suit, evidenced by the progressive reduction in growth of T4-2 cells seeded on either shCtrl (tip^{high})-, shCtrl:shNotch1 chimera (sh1:1)- or shNotch1 (tip^{low})-EC cultures (Fig. 5d, e). The percentage of quiescent tumor clusters also increased modestly in cultures that contained fewer neovascular tips (Fig. 5f).

We tested also whether increased neovascular tip concentration would promote tumor cell growth in culture and *in vivo*. To enrich for neovascular tips in culture, we allowed microvascular networks to develop for only 3 days prior to seeding T4-2 cells. The number of neovascular tips at day 3 of network formation was nearly double that of day 7 cultures (Supplemental Fig. 5a, b, e). Seeding tumor cells at each of these developmental time points and measuring growth 10 days later confirmed that BCC growth correlates positively with endothelial tip number; T4-2 cells grew nearly *6-times* more when seeded on networks rich in neovascular tips, and significantly fewer of these tumor clusters became quiescent (Supplemental Fig. 5c, d, f, g).

To test whether a microenvironment rich in neovascular tips promotes tumor cell growth *in vivo*, we utilized zebrafish with a mutation in the gene encoding microsomal triglyceride transfer protein (*mtp*). These mutants, called *stalactite*, have an ectopic microvascular sprouting phenotype that is especially pronounced in the perivitelline/subintestinal space at 3.5 days post-fertilization (dpf)[31]. Accordingly, we injected ~1–10 MDA-MB-231 cells expressing mCherry into the subintestinal space of wild-type (WT) and *mtp−/−* mutant zebrafish at this timepoint. Fish injected unsuccessfully, defined as those lacking red fluorescence in the subintestinal space, or those over-injected (an area fraction of red fluorescence over a pre-determined threshold value), were discounted from further analysis. Successfully injected zebrafish were imaged four days later (7.5dpf; *mtp−/−* mutants perish shortly thereafter[31]—Fig. 6a). On average, *mtp−/−* mutants had 4-times more neovascular sprouts than their WT siblings at the time of injection (Fig. 6b–d). In WT fish that survived until 7.5dpf and had viable MDA-MB-231 cells in their subintestinal space, those that adhered to subintestinal vessels did not grow appreciably (Fig. 6e, g; note that for each fish, tumor cell area fraction at 7.5 dpf was normalized to the corresponding value obtained just after injection to account for variations in initial seeding density). In contrast, tumor cells injected into the subintestinal space of *mtp−/−* mutants expanded significantly more than those in WT siblings, particularly in the vicinity of neovascular tips (Fig. 6f, g).

Neovascular tips constitute 'micrometastatic niches' rich in periostin and active TGF-β1

The above experiments confirmed that neovascular tips promote tumor cell outgrowth in organotypic culture and *in vivo*, implying production of distinct tumor-promoting factors by neovascular tip cells. To identify factors enriched around neovascular tips, we utilized tandem mass spectrometry and compared decellularized ECM from neovascular tip^{high}

(shCtrl) and tip^{low} (shNotch1) cultures (Fig. 5a). Tip^{high} cultures were characterized by enhanced expression of POSTN, tenascin, versican, and fibronectin (Fig. 7a), all molecules involved in formation of the metastatic niche[5,32–35]. Further, tip^{high} cultures exhibited reduced expression of molecules involved in sequestering another known mediator of metastatic outgrowth, TGF-β1 (biglycan and LTBP1, Fig. 7a) [36], suggesting that active TGF-β1 itself would be expressed more highly at neovascular tips. Immunofluorescent staining of E4-ECs in 3D co-cultures confirmed that active TGF-β1 and POSTN were expressed highly at neovascular tips (Fig. 7b, c, e). In contrast, latent TGF-β1 was expressed prominently in endothelial stalks (Fig. 7d). These findings were confirmed *in vivo* in physiologic and pathologic settings. POSTN and active TGF-β1 were concentrated on/near endothelial tip cells in the developing mouse retina (Supplemental Fig. 6a, c, e), but were not detected consistently around established 'phalanx' endothelium in the same tissue (Supplemental Fig. 6c, e; insets). Examining established metastases revealed that in this setting, POSTN and active TGF-β1 were deposited prominently around endothelial tip cells as well (Supplemental Fig. 6b, d, f). In contrast, expression of both factors near non-tumor-associated endothelium within the same tissue sections was diminished (Supplemental Fig. 6d, f; insets). Pulsing POSTN and TGF-β1 into microvascular niche cultures to recapitulate a tip-enriched microenvironment promoted BCC growth; T4-2 cells seeded upon lung-like microvascular niches and treated transiently with POSTN and TGF-β1 (twice over the first 48h to mimic the brief interaction of tumor cells with neovascular tips) experienced 3-times more outgrowth when compared to vehicle treated counterparts (Fig. 7f–h). This finding confirms that POSTN and TGF-β1, which are expressed highly at neovascular tips, promote BCC outgrowth within a tumor suppressive microenvironment.

Discussion

Using murine models, zebrafish and organotypic microvascular niches composed of human cells, we demonstrate here that: i) dormant DTCs from the breast reside on or near lung and BoMa microvasculature *in vivo*, ii) stable microvasculature constitutes a dormant niche that induces sustained tumor cell quiescence via TSP-1, and iii) the tumor-suppressive nature of microvascular endothelium is lost at sprouting endothelial tips, which are characterized by reduced TSP-1 expression and enhanced expression of pro-tumor factors POSTN and TGF-β1 (Fig. 7i). Studies of primary tumors have focused primarily on the tumor's regulation of the endothelium. We believe this paradigm now shifts at secondary sites, where DTCs are the minority constituent of the tissue and subject to direct control by microvascular endothelium and perhaps other resident cell types.

The notion that ECs directly regulate cells in the perivascular microenvironment is rooted in a number of biological studies on normal tissues (*reviewed in* [25]). ECs with phenotypic characteristics of neovascular tip cells spark growth and morphogenesis of the liver[37] and regeneration of lung alveoli[38]. On the other hand, established endothelium promotes pancreatic differentiation[39], inhibits smooth muscle cell proliferation[40] and maintains pluripotency of neural, hematopoietic and mesenchymal stem cells[23,41–44]. Our study demonstrates that this scenario— that mature microvasculature confers tissue quiescence and sprouting endothelium promotes tissue growth— is at work also in the DTC

microenvironment. These findings may apply generally to primary tumors also, thus shedding light on the apparent dichotomy of EC function at the primary site[45–49].

The therapeutic implications of our results are multi-fold. Foremost is that identification of tumor-suppressive factors derived from stable endothelium may guide therapies designed to enforce DTC dormancy. This raises the question of whether other molecules in the microvascular BM function as tumor suppressors, and whether these can be used in combination with TSP-1 to stave off metastatic relapse. Second is that factors enriched in neovascular sub-niches may be targeted early in tumor progression to prevent establishment of micro-metastatic niches that disrupt DTC quiescence. In this regard, our study complements prior work pinpointing POSTN, TGF-β1 and other molecules as potential therapeutic targets[5,32–36], and reveals further that these molecules arise from an unexpected source, namely neovascular endothelium.

Surprisingly, many of the factors upregulated in neovascular tip-enriched cultures are documented components of pre-metastatic and metastatic niches [5,7,32–34]. Given the nature of our results, this provides further evidence for the *in vivo* relevance of our model systems, but also raises a number of questions. What is the origin of this commonality? Does it reflect a tight interconnectedness of metastatic niche formation on the induction of neovasculature? It is interesting to note that nascent endothelium was recently shown to initiate a Th2-mediated inflammatory response in asthma[50], a response that is also associated with accelerated metastatic outgrowth in tumor models[51–53]. Thus, by direct deposition of tumor promoting factors, as well as by secreting cytokines that stimulate macrophage polarization to a pro-tumor phenotype[50,53], neovascular tips may function as a nexus that directly and indirectly catalyzes formation of a micrometastatic niche. Accordingly, long-term administration of drugs aimed at preventing neovascular formation[54] through inhibition of VEGFR2- [55] or integrin $\alpha_v\beta_3$-[56] driven signaling, or by targeting more recently discovered pro-angiogenic signaling mechanisms[57], may prove effective in delaying relapse of early stage breast cancer patients. We believe that it will be crucial to deliver these drugs in a manner that prevents cultivation of the pro-tumor neovascular niche while preserving the dormant niche fostered by stable microvasculature.

It remains to be determined whether the mechanisms we have identified here apply also to other tumor types and in other secondary tissues. We propose that a systemic understanding of interactions between DTCs and their microenvironment will provide a vehicle by which we can design more effective therapies to keep DTCs at bay—or eradicate them—in early-stage cancer patients.

Supplementary Material

Refer to Web version on PubMed Central for supplementary material.

Acknowledgments

We thank S. Rafii and B. Weinstein for generously providing *E4ORF1* lentiviral plasmid and *stalactite* mutant zebrafish, respectively. We are grateful to N. Boudreau, S. Rafii, R. Schwartz, R. Xu, A. Bruni-Cardoso and A.L. Correia for critical insight, and to other current members of the Bissell laboratory for helpful discussions. We thank A. Lo and C. Williams for technical assistance and T. Varimezova for performing blinded quantitative analysis.

C.M.G. was funded by a Glenn T. Seaborg Postdoctoral Fellowship from LBNL and by a NCI-U54CA143836 training grant. K.J.E. is a Robert Black Fellow supported by the Damon Runyon Cancer Research Foundation (DRG-109-10). K.A.H.'s laboratory is supported by grants from the NIH (R01HL042493 and R01HL090895) and from the March of Dimes Foundation (6-FY12-356). The work in D.Y.R.S.'s laboratory was funded in part by grants from the NIH (HL54737) and the Packard Foundation. E.C.'s laboratory is supported by a shared instrument grant (NIH/NCRR 1 S10 RR023680-1) and a DOE Subcontract (DE-AC02-05CH1123) from LBNL. The work from M.J.B.'s laboratory is supported by grants from the U.S. Department of Energy, Office of Biological and Environmental Research and Low Dose Scientific Focus Area (contract no. DE-AC02-05CH1123); by National Cancer Institute (awards U01CA169538 (to D.L. and M.J.B.), U54CA126552, R37CA064786, and U54CA143836-- Bay Area Physical Sciences–Oncology Center, University of California, Berkeley, California); by a grant from the Breast Cancer Research Foundation; and by U.S. Department of Defense (W81XWH0810736).

References

1. Aguirre-Ghiso JA. Models, mechanisms and clinical evidence for cancer dormancy. Nat Rev Cancer. 2007; 7:834–846. [PubMed: 17957189]
2. Goss PE, Chambers AF. Does tumour dormancy offer a therapeutic target? Nat Rev Cancer. 2010; 10:871–877. [PubMed: 21048784]
3. Klein CA. Parallel progression of primary tumours and metastases. Nat Rev Cancer. 2009; 9:302–312. [PubMed: 19308069]
4. Uhr JW, Pantel K. Controversies in clinical cancer dormancy. Proc Natl Acad Sci U S A. 2011; 108:12396–12400. [PubMed: 21746894]
5. Kaplan RN, et al. VEGFR1-positive haematopoietic bone marrow progenitors initiate the pre-metastatic niche. Nature. 2005; 438:820–827. [PubMed: 16341007]
6. Peinado H, et al. Melanoma exosomes educate bone marrow progenitor cells toward a pro-metastatic phenotype through MET. Nat Med. 2012; 18:883–891. [PubMed: 22635005]
7. Psaila B, Lyden D. The metastatic niche: adapting the foreign soil. Nat Rev Cancer. 2009; 9:285–293. [PubMed: 19308068]
8. Suzuki M, Mose ES, Montel V, Tarin D. Dormant cancer cells retrieved from metastasis-free organs regain tumorigenic and metastatic potency. Am J Pathol. 2006; 169:673–681. [PubMed: 16877365]
9. Naumov GN, et al. Persistence of solitary mammary carcinoma cells in a secondary site: a possible contributor to dormancy. Cancer Res. 2002; 62:2162–2168. [PubMed: 11929839]
10. Pantel K, et al. Differential expression of proliferation-associated molecules in individual micrometastatic carcinoma cells. J Natl Cancer Inst. 1993; 85:1419–1424. [PubMed: 7688814]
11. Bissell MJ, Hines WC. Why don't we get more cancer? A proposed role of the microenvironment in restraining cancer progression. Nat Med. 2011; 17:320–329. [PubMed: 21383745]
12. Boudreau N, Sympson CJ, Werb Z, Bissell MJ. Suppression of ICE and apoptosis in mammary epithelial cells by extracellular matrix. Science. 1995; 267:891–893. [PubMed: 7531366]
13. Spencer VA, et al. Depletion of nuclear actin is a key mediator of quiescence in epithelial cells. J Cell Sci. 2011; 124:123–132. [PubMed: 21172822]
14. Weaver VM, et al. beta4 integrin-dependent formation of polarized three-dimensional architecture confers resistance to apoptosis in normal and malignant mammary epithelium. Cancer Cell. 2002; 2:205–216. [PubMed: 12242153]
15. Weaver VM, et al. Reversion of the malignant phenotype of human breast cells in three-dimensional culture and in vivo by integrin blocking antibodies. J Cell Biol. 1997; 137:231–245. [PubMed: 9105051]
16. Bissell MJ, Hall HG, Parry G. How does the extracellular matrix direct gene expression? J Theor Biol. 1982; 99:31–68. [PubMed: 6892044]
17. Petersen OW, Ronnov-Jessen L, Howlett AR, Bissell MJ. Interaction with basement membrane serves to rapidly distinguish growth and differentiation pattern of normal and malignant human breast epithelial cells. Proc Natl Acad Sci U S A. 1992; 89:9064–9068. [PubMed: 1384042]
18. Braun S, et al. A pooled analysis of bone marrow micrometastasis in breast cancer. N Engl J Med. 2005; 353:793–802. [PubMed: 16120859]
19. Chambers AF, Groom AC, MacDonald IC. Dissemination and growth of cancer cells in metastatic sites. Nat Rev Cancer. 2002; 2:563–572. [PubMed: 12154349]

20. Francia G, Cruz-Munoz W, Man S, Xu P, Kerbel RS. Mouse models of advanced spontaneous metastasis for experimental therapeutics. Nat Rev Cancer. 2011; 11:135–141. [PubMed: 21258397]
21. Paget S. The distribution of secondary growths in cancer of the breast. 1889. Cancer Metastasis Rev. 1989; 8:98–101. [PubMed: 2673568]
22. Briand P, Nielsen KV, Madsen MW, Petersen OW. Trisomy 7p and malignant transformation of human breast epithelial cells following epidermal growth factor withdrawal. Cancer Res. 1996; 56:2039–2044. [PubMed: 8616848]
23. Butler JM, et al. Endothelial cells are essential for the self-renewal and repopulation of Notch-dependent hematopoietic stem cells. Cell Stem Cell. 2010; 6:251–264. [PubMed: 20207228]
24. Seandel M, et al. Generation of a functional and durable vascular niche by the adenoviral E4ORF1 gene. Proc Natl Acad Sci U S A. 2008; 105:19288–19293. [PubMed: 19036927]
25. Butler JM, Kobayashi H, Rafii S. Instructive role of the vascular niche in promoting tumour growth and tissue repair by angiocrine factors. Nat Rev Cancer. 2010; 10:138–146. [PubMed: 20094048]
26. Evensen L, et al. Mural cell associated VEGF is required for organotypic vessel formation. PLoS One. 2009; 4:e5798. [PubMed: 19495422]
27. Weinstat-Saslow DL, et al. Transfection of thrombospondin 1 complementary DNA into a human breast carcinoma cell line reduces primary tumor growth, metastatic potential, and angiogenesis. Cancer Res. 1994; 54:6504–6511. [PubMed: 7527299]
28. Roberts DD. Regulation of tumor growth and metastasis by thrombospondin-1. FASEB J. 1996; 10:1183–1191. [PubMed: 8751720]
29. Ghajar CM, et al. The effect of matrix density on the regulation of 3-D capillary morphogenesis. Biophys J. 2008; 94:1930–1941. [PubMed: 17993494]
30. Hellstrom M, et al. Dll4 signalling through Notch1 regulates formation of tip cells during angiogenesis. Nature. 2007; 445:776–780. [PubMed: 17259973]
31. Avraham-Davidi I, et al. ApoB-containing lipoproteins regulate angiogenesis by modulating expression of VEGF receptor 1. Nat Med. 2012; 18:967–973. [PubMed: 22581286]
32. Kim S, et al. Carcinoma-produced factors activate myeloid cells through TLR2 to stimulate metastasis. Nature. 2009; 457:102–106. [PubMed: 19122641]
33. Malanchi I, et al. Interactions between cancer stem cells and their niche govern metastatic colonization. Nature. 2012; 481:85–89. [PubMed: 22158103]
34. Oskarsson T, et al. Breast cancer cells produce tenascin C as a metastatic niche component to colonize the lungs. Nat Med. 2011; 17:867–874. [PubMed: 21706029]
35. Soikkeli J, et al. Metastatic outgrowth encompasses COL-I, FN1, and POSTN up-regulation and assembly to fibrillar networks regulating cell adhesion, migration, and growth. Am J Pathol. 2010; 177:387–403. [PubMed: 20489157]
36. Bierie B, Moses HL. Tumour microenvironment: TGFbeta: the molecular Jekyll and Hyde of cancer. Nat Rev Cancer. 2006; 6:506–520. [PubMed: 16794634]
37. Matsumoto K, Yoshitomi H, Rossant J, Zaret KS. Liver organogenesis promoted by endothelial cells prior to vascular function. Science. 2001; 294:559–563. [PubMed: 11577199]
38. Ding BS, et al. Endothelial-derived angiocrine signals induce and sustain regenerative lung alveolarization. Cell. 2011; 147:539–553. [PubMed: 22036563]
39. Lammert E, Cleaver O, Melton D. Induction of pancreatic differentiation by signals from blood vessels. Science. 2001; 294:564–567. [PubMed: 11577200]
40. Dodge AB, Lu X, D'Amore PA. Density-dependent endothelial cell production of an inhibitor of smooth muscle cell growth. J Cell Biochem. 1993; 53:21–31. [PubMed: 8227180]
41. Crisan M, et al. A perivascular origin for mesenchymal stem cells in multiple human organs. Cell Stem Cell. 2008; 3:301–313. [PubMed: 18786417]
42. Kobayashi H, et al. Angiocrine factors from Akt-activated endothelial cells balance self-renewal and differentiation of haematopoietic stem cells. Nat Cell Biol. 2010; 12:1046–1056. [PubMed: 20972423]

43. Shen Q, et al. Endothelial cells stimulate self-renewal and expand neurogenesis of neural stem cells. Science. 2004; 304:1338–1340. [PubMed: 15060285]
44. Ding L, Saunders TL, Enikolopov G, Morrison SJ. Endothelial and perivascular cells maintain haematopoietic stem cells. Nature. 2012; 481:457–462. [PubMed: 22281595]
45. Bandyopadhyay S, et al. Interaction of KAI1 on tumor cells with DARC on vascular endothelium leads to metastasis suppression. Nat Med. 2006; 12:933–938. [PubMed: 16862154]
46. Calabrese C, et al. A perivascular niche for brain tumor stem cells. Cancer Cell. 2007; 11:69–82. [PubMed: 17222791]
47. Franses JW, Baker AB, Chitalia VC, Edelman ER. Stromal endothelial cells directly influence cancer progression. Sci Transl Med. 2011; 3:66ra65.
48. Indraccolo S, et al. Cross-talk between tumor and endothelial cells involving the Notch3-Dll4 interaction marks escape from tumor dormancy. Cancer Res. 2009; 69:1314–1323. [PubMed: 19208840]
49. Panigrahy D, et al. Epoxyeicosanoids stimulate multiorgan metastasis and tumor dormancy escape in mice. J Clin Invest. 2012; 122:178–191. [PubMed: 22182838]
50. Asosingh K, et al. Nascent endothelium initiates th2 polarization of asthma. J Immunol. 2013; 190:3458–3465. [PubMed: 23427249]
51. Lin EY, Nguyen AV, Russell RG, Pollard JW. Colony-stimulating factor 1 promotes progression of mammary tumors to malignancy. J Exp Med. 2001; 193:727–740. [PubMed: 11257139]
52. Qian BZ, Pollard JW. Macrophage diversity enhances tumor progression and metastasis. Cell. 2010; 141:39–51. [PubMed: 20371344]
53. DeNardo DG, et al. CD4(+) T cells regulate pulmonary metastasis of mammary carcinomas by enhancing protumor properties of macrophages. Cancer Cell. 2009; 16:91–102. [PubMed: 19647220]
54. Folkman J. Angiogenesis: an organizing principle for drug discovery? Nat Rev Drug Discov. 2007; 6:273–286. [PubMed: 17396134]
55. Jakobsson L, et al. Endothelial cells dynamically compete for the tip cell position during angiogenic sprouting. Nat Cell Biol. 2010; 12:943–953. [PubMed: 20871601]
56. Brooks PC, Clark RA, Cheresh DA. Requirement of vascular integrin alpha v beta 3 for angiogenesis. Science. 1994; 264:569–571. [PubMed: 7512751]
57. Stratman AN, Davis MJ, Davis GE. VEGF and FGF prime vascular tube morphogenesis and sprouting directed by hematopoietic stem cell cytokines. Blood. 2011; 117:3709–3719. [PubMed: 21239704]

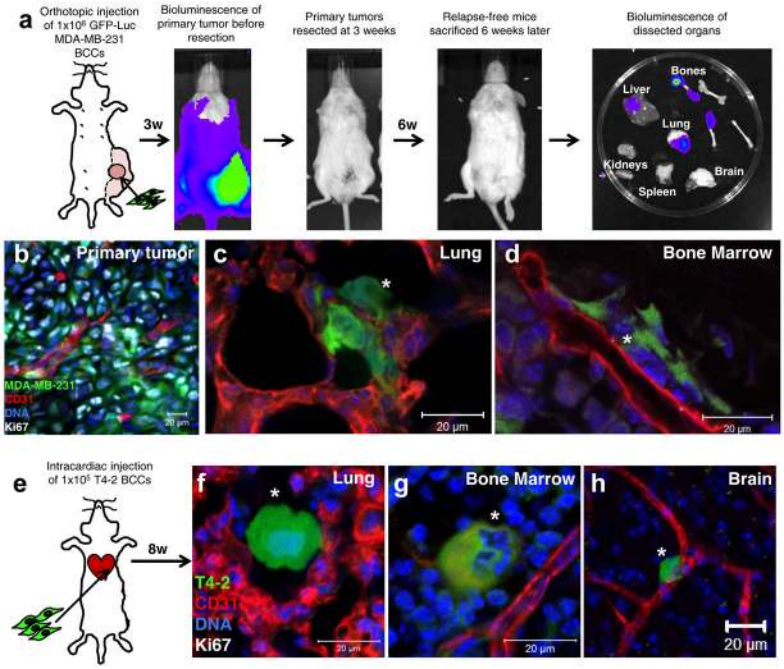

Figure 1.

Dormant breast tumor cells reside on microvascular endothelium in distant tissues *in vivo*. (**a**) GFP-Luc MDA-MB-231 cells were injected into the inguinal mammary gland of NOD-SCID mice. Tumors were resected at 3 wks (V_{avg} = 0.5 cm^3; representative bioluminescence shown). Mice that were relapse-free after 6 wks (4/20 mice) were sacrificed and visceral organs were dissected. (**b**) Representative image of a primary tumor section fixed and stained for endothelial-specific marker CD31 (red), and cell cycle marker Ki67 (white). DNA was labeled with Hoechst 33342 (blue). Dormant (Ki67-negative) DTCs (white asterisks) were found residing on microvascular endothelium in (**c**) lung and (**d**) BoMa tissues isolated from mice sacrificed 6 wks after primary tumor resection. (**e**) mCherry T4-2 cells (false-colored green here for consistency) were introduced via intra-cardiac injection, and mice that did not show any evidence of metastatic burden were sacrificed 8 wks later. In this second model, dormant (Ki-67 negative) T4-2 BCCs (white asterisks) also were found residing perivascularly in (**f**) lung, (**g**) bone marrow, and (**h**) brain. Scale bars = 20 μm.

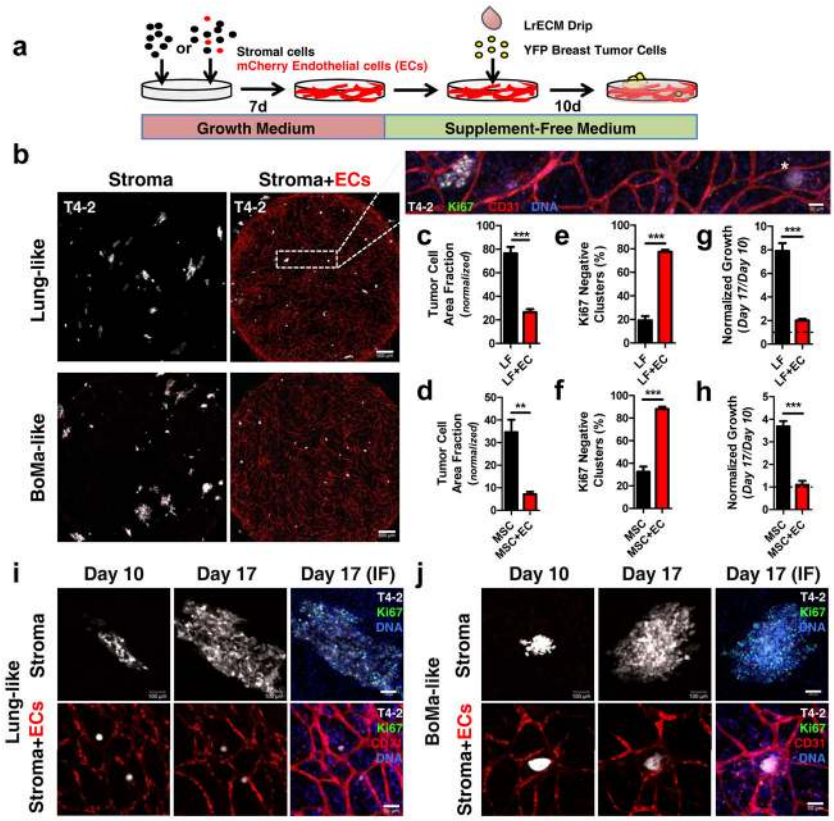

Figure 2.

Microvascular endothelium induces sustained quiescence of breast tumor cells in engineered cultures. (**a**) Lung and BoMa stroma (LFs and MSCs, respectively) were seeded alone or with mCherry-E4-ECs. In co-culture, mCherry-E4-ECs self-assembled into 3D microvascular networks over 7d. YFP-expressing BCCs (T4-2) were then seeded sparsely (240/cm^2) in SFM onto stroma or microvascular niche cultures and overlaid with a drip of laminin-rich ECM (LrECM) diluted in media to provide BCCs with a 3D microenvironment[64]. Entire wells were imaged 10 days later. (**b**) Representative images of T4-2 cell growth within lung-like or BoMa-like niches containing stroma only, or stroma + ECs, 10 days post-seeding. Scale bars = 500 μm. (**c, d**) Tumor cell area fraction of YFP T4-2 at day 10 (normalized by value measured immediately post-seeding to correct for any minor variations in initial seeding density) in lung-like or BoMa-like niches, respectively (n=5 sets of co-cultures analyzed per condition). Error bars denote s.e.m. **p=0.001 and ***p<0.0001 by two-tailed t test. Day 10 co-cultures were fixed and stained for CD31 to label ECs and Ki67 to identify actively cycling tumor cells (**b**, inset; Scale bar = 50 μm). The percentage of Ki67-negative clusters (*white asterisk* in **b**, inset) was quantified for T4-2 cells seeded on (**e**) lung- and (**f**) BoMa-like niches (n=5 sets of co-cultures analyzed per condition). Error bars denote s.e.m. *** p<0.0001 by two-tailed t test. Tumor cell growth was measured over an additional 7 days (day 17 normalized by day 10) in (**g**) lung- and (**h**) BoMa-like niches to determine whether quiescent tumor clusters at day 10 remained quiescent (n=5 sets of co-cultures analyzed per condition). Error bars denote s.e.m. *** p<0.0001 by two-tailed t test. Live images of representative T4-2 cells on (**i**) lung-like stroma and microvascular niche are

shown for day 10 and day 17, with IF staining to confirm Ki67 status. (**j**) The same is shown for representative T4-2 cells on BoMa-like stroma and microvascular niche cultures. Note that stroma culture scale bars = 100 μm and microvascular niche culture scale bars = 50 μm.

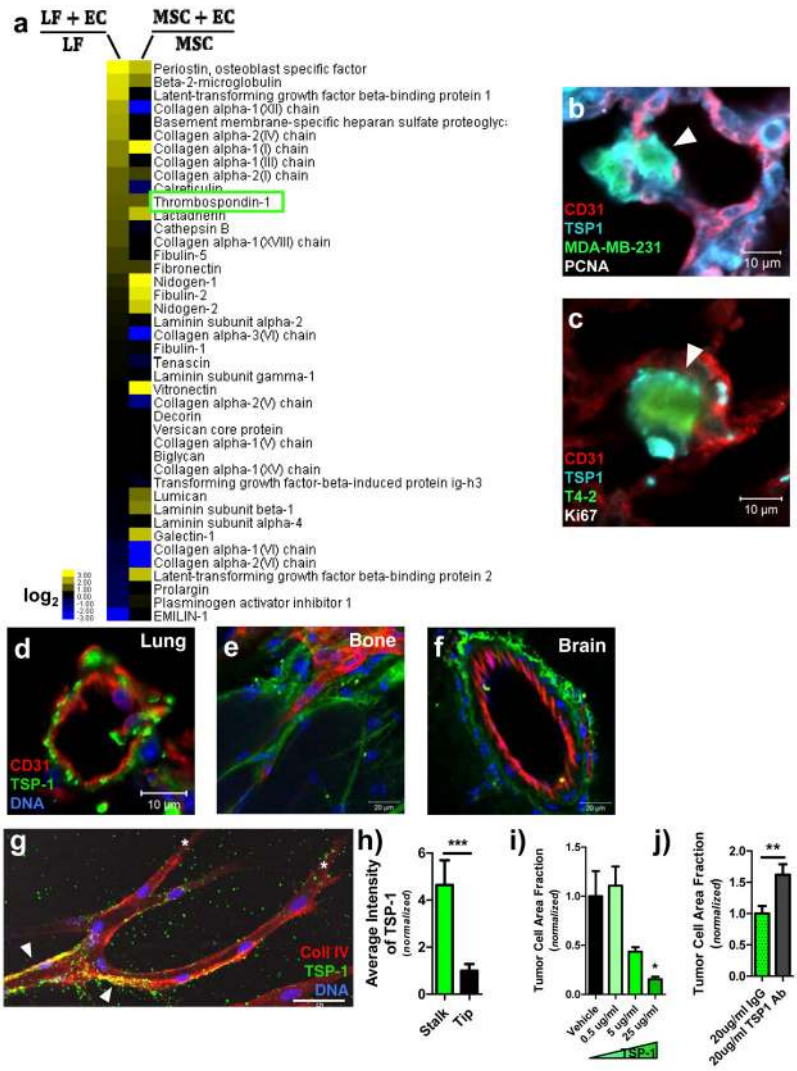

Figure 3.

Thrombospondin-1 is an angiocrine tumor suppressor. Lung- and BoMa-like stroma and microvascular niche cultures were decellularized and residual proteins were acid extracted and subjected to LC-MS/MS analysis. (**a**) Heatmap of ECM proteins (spectral counts) from lung-like microvascular niche (LF + EC) normalized by lung stroma (LF; sorted high to low) and BoMa-like microvascular niche (MSC + EC) normalized by BoMa stroma (MSC). Log_2 intensity scale shown at lower left. Localized expression of TSP-1 at the interface between dormant DTCs and lung microvasculature was confirmed in (**b**) spontaneous and (**c**) experimental metastasis models (*white arrowheads*). Scale bars = 10 μm. TSP-1 localization to the vascular BM was also confirmed in non-tumor bearing mice in (**d**) lung, (**e**) bone and (**f**) brain. Scale bars: 10 μm for lung, 20 μm for others. (**g**) Endothelial source of TSP-1 was confirmed by utilizing a 3D model of capillary morphogenesis where sprouting ECs are separated from inductive LFs by several millimeters. TSP-1 colocalized with type IV collagen in the BM of established microvessel stalks (*white arrowheads*), but TSP-1 appeared to be downregulated at neovascular tips (*white asterisks*). Scale bar = 50 μm. This was confirmed by (**h**) quantification of TSP-1 intensity at stalks vs. tips (n=16

microvessels pooled from 3 different experiments). Error bars denote s.e.m. ***p=0.0005 by two-tailed paired t-test. (**i**) Add-back of TSP-1 to T4-2 cells plated on lung stroma effectively substituted for the presence of ECs by causing a significant reduction in tumor cell growth (normalized to vehicle condition; n=3 sets of co-cultures analyzed per condition). Error bars denote s.e.m. * p<0.05 when compared to Vehicle by one-way ANOVA and Dunnett's multiple comparisons test. (**j**) Treating lung-like microvascular niches with a TSP-1 blocking antibody resulted in significantly enhanced tumor cell growth (vs. IgG control; n=5 sets of co-cultures analyzed per condition). Error bars denote s.e.m. **p=0.0054 by two-tailed unpaired t-test.

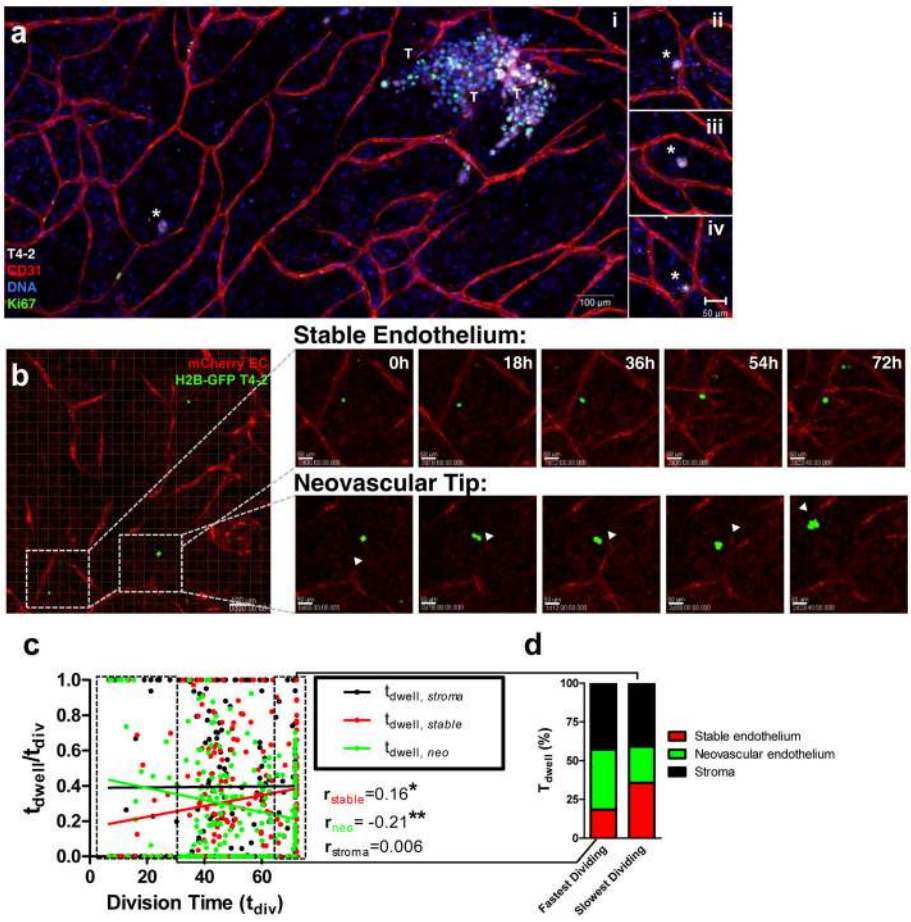

Figure 4.

Opposite regulation of tumor dormancy and growth by endothelial sub-niches: stable endothelium inhibits—whereas neovascular tips promote—breast tumor cell growth. (**ai**) Immunofluorescence of YFP T4-2 on BoMa-like microvascular niche after 10d. *: Ki67-negative tumor cluster; T: neovascular tips surrounding proliferative tumor. Scale bar = 100 μm. Insets **ii–iv**: additional examples of Ki67-negative BCCs residing on/near microvasculature from that *same culture* shown in (**ai**). Scale bar = 50 μm. (**b**) Stills from live tracking of histone H2B-GFP T4-2 cells on BoMa-like microvascular sub-niches (stable endothelium and neovascular tip) from 0–72h (see also Supplemental Movies 1–2). White arrowheads denote approaching tip and subsequent T4-2 division. Scale bars: left-most panel= 100 μm, right panels= 50 μm. (**c**) Scatter plot of T4-2 cell dwell time fraction (t_{dwell}/t_{div}) within stable ($t_{dwell,\ stable}$), neovascular ($t_{dwell,\ neo}$) or stromal ($t_{dwell,\ stroma}$) sub-niches vs. division time (t_{div}, n= 229 cells pooled from 3 separate time-lapse experiments). Pearson correlation analysis yielded significant correlation of $t_{dwell,\ \textit{stable}}$ with t_{div} and significant anti-correlation of $t_{dwell,\ \textit{neo}}$ with t_{div}, meaning that BCCs with longer division times tended to dwell *more* around stable endothelium and *less* around neovascular tips. Pearson coefficients (r) for stable endothelium, neovascular tips, and stroma are listed to right of plot. * p= 0.014 and ** p= 0.001 (two-tailed). (**d**) Dwell time (% of time to first division) as a function of sub-niche for fastest dividing tumor cells ($t < t_{avg} - SD$; n=30 cells) and slowest dividing tumor cells ($t > t_{avg} + SD$; n=59 cells).

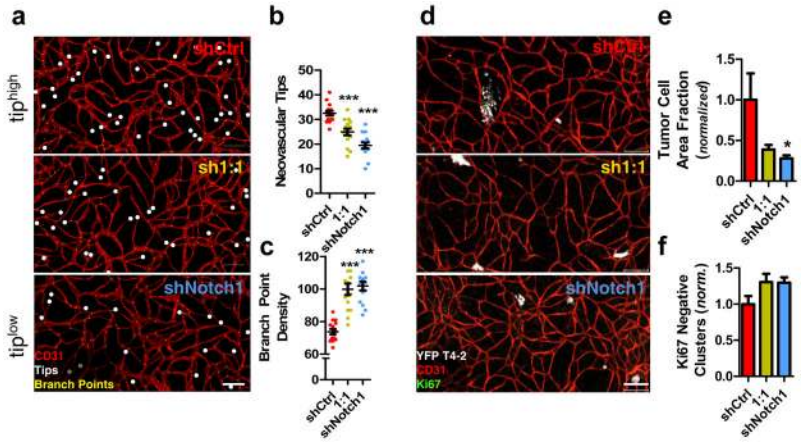

Figure 5.

Notch1-mediated reduction in neovascular tips suppresses breast tumor cell outgrowth. Microvascular niches were created with stromal cells mixed with shCtrl E4-EC and/or shNotch1 E4-EC. YFP T4-2 cells were then seeded in SFM and growth was analyzed 10 days later. (**a**) Microvascular niches composed of shCtrl E4-EC, shNotch1 E4-EC, or a 1:1 mix of the two ('sh1:1') were fixed and stained for CD31 at day 7. Scale bar = 200 μm. (**b**) Neovascular tip number/field (large white dots in **a**) and (**c**) branch point density (small yellow dots in **a**) were quantified (n=15 fields of microvascular networks pooled from 5 separate co-cultures). Error bars denote s.e.m ***p<0.001 when compared to shCtrl condition by one-way ANOVA and Dunnett's post-test. (**d**) Representative images of YFP T4-2 seeded upon shCtrl EC, shNotch1 EC, or sh1:1 cultures, fixed and stained for CD31 and Ki67 10d post-seeding. Scale bar = 200 μm. (**e**) Quantification of normalized tumor cell area fraction and (**f**) %Ki67-negative clusters (each normalized by shCtrl condition; n=5 sets of co-cultures analyzed per condition). Error bars denote s.e.m. *p<0.05 when compared to shCtrl condition by one-way ANOVA and Dunnett's post-test in (**e**).

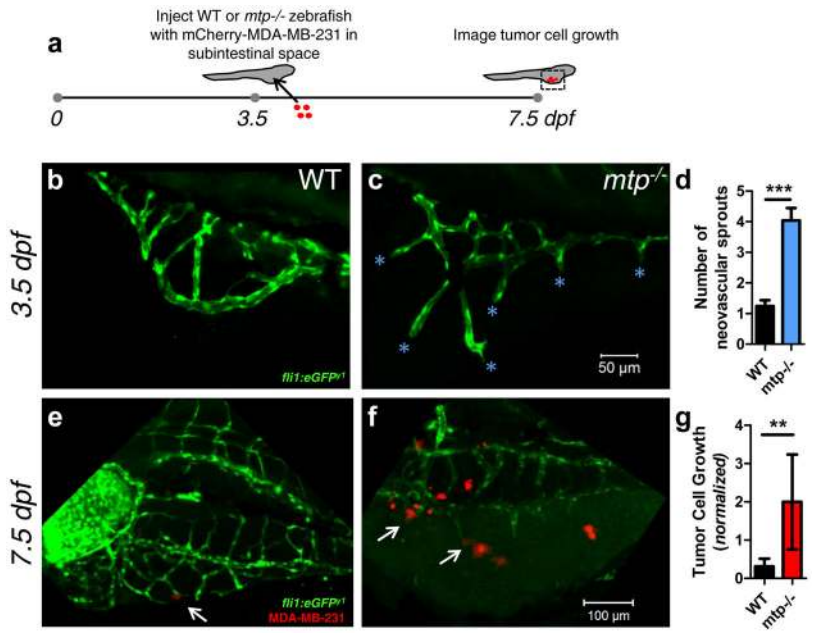

Figure 6.

Ectopic vascular sprouting promotes growth of injected breast tumor cells in zebrafish larvae. (**a**) ~1–10 mCherry-MDA-MB-231 BCCs were injected into the subintestinal space of 3.5 dpf *mtp−/−* mutant zebrafish and WT siblings (both containing the *fli1:eGFP* transgene) and imaged 4 days later. The injection time point (3.5 dpf) was chosen because (**b**) WT subintestinal vessels had few sprouts by this time point, while (**c**) the ectopic sprouting phenotype of the *mtp−/−* mutant was exaggerated (*cyan asterisks* denote neovascular sprouts). Scale bar = 50 μm. (**d**) Quantification of ectopic/neovascular sprouts in subintestinal space of WT and *mtp−/−* mutant siblings (n=25 WT zebrafish analyzed; n=23 *mtp−/−* zebrafish analyzed). Error bars denote s.e.m. ***p<0.0001 by two-tailed unpaired t-test. Representative images of (**e**) WT and (**f**) *mtp−/−* mutant zebrafish 4 days post-injection (i.e., 7.5 dpf) with mCherry-MDA-MB-231 cells. Scale bar = 100 μm. White arrow in (**e**) points to small cluster on abluminal surface of subintestinal vessel of WT, while white arrows in (**f**) point to larger clusters localized to neovascular tips in *mtp−/−* mutant. (**g**) Tumor cell area fraction in the subintestinal space was quantified at 7.5 dpf and normalized to the corresponding value post-injection for each surviving zebrafish with viable tumor cells in its subintestinal space to account for any variations in injection density (n=16 WT zebrafish analyzed; n=9 *mtp−/−* zebrafish analyzed). Error bars denote s.e.m. **p=0.005 by Mann-Whitney test.

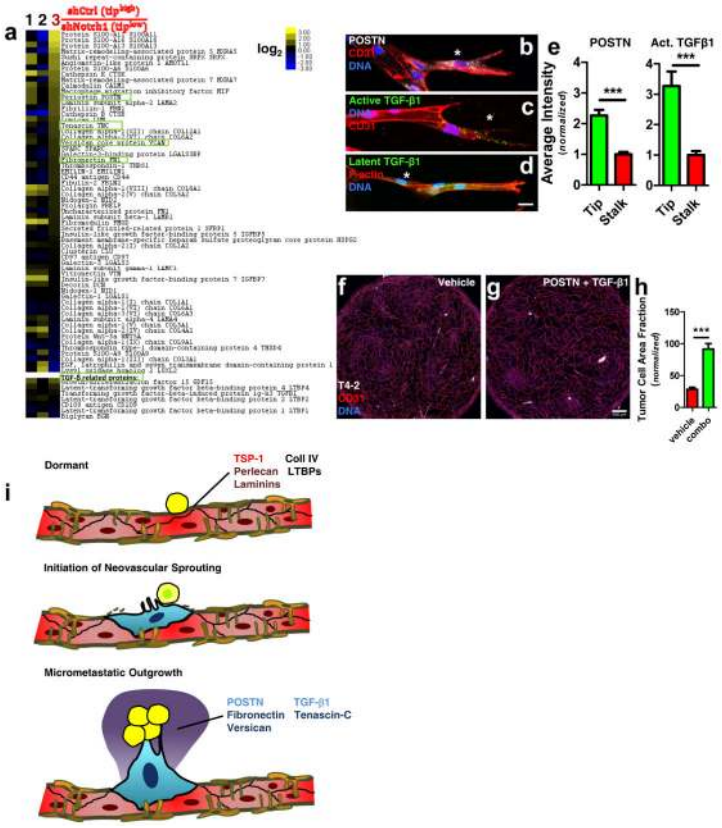

Figure 7.

Neovascular tips comprise 'micrometastatic niches' enriched for POSTN and TGF-β1. (**a**) Heatmap of ECM proteins (spectral counts) from **1**) neovascular tip^{high} cultures (LF + shCtrl EC) normalized by lung stroma (LF), **2**) neovascular tip^{low} cultures (LF + shNotch1 EC) normalized by lung stroma (LF), and **3**) tip^{high} cultures normalized by tip^{low} cultures (sorted high to low with respect to this comparison, $\log_2$ scale). Representative images of microvessels stained for (**b**) POSTN, (**c**) active TGF-β1 and (**d**) latent TGF-β1. Scale bar = 20 μm. (**e**) Quantification of relative POSTN (*left*) and active TGF-β1 intensity (*right*) at the tip vs. stalk of microvessels (n=15 microvessels were pooled from 3 different experiments for analysis of POSTN intensity quantification; n=16 microvessels were pooled and analyzed for active TGF-β1 intensity quantification). Error bars represent s.e.m. ***p<0.0001 by paired two-tailed t-test. Representative images of microvascular niche cultures seeded with T4-2 cells and treated with (**f**) vehicle or (**g**) a combination of POSTN (50 ng/ml) and TGF-β1 (10 pg/ml) twice over the first 48h, and imaged at day 10. Scale bar = 500 μm. (**h**) Normalized tumor cell area fraction of YFP T4-2 at day 10 treated by vehicle or by said combination of POSTN and TGF-β1 ('combo'; n=5 sets of co-cultures analyzed per condition). Error bars represent s.e.m. ***p<0.0001 by two-tailed t test. (**i**) A visual summary of our findings: In distant microenvironments, single or small clusters of DTCs reside in the perivascular niche and are maintained in a quiescent state by endothelial-derived factors. Here, we have identified TSP-1 as one such factor, while perlecan was identified by others as an EC-derived factor that suppresses tumor growth[47]. Other ECM molecules such as laminins, type IV collagen and latent TGF-β binding proteins (LTBPs)

may contribute directly or indirectly to the dormant niche. As vascular homeostasis is disrupted with induction of neovascular sprouting, endothelial architecture is perturbed. The result is not only loss of suppressive signals (e.g., TSP-1), but deposition of ECM molecules and growth factors that promote micrometastatic outgrowth. Thus, maintaining vascular homeostasis could be the key to sustaining DTC dormancy long-term.